JBC RESEARCH ARTICLE

The multidomain architecture of a bacteriophage endolysin enables intramolecular synergism and regulation of bacterial lysis

Received for publication, December 1, 2020, and in revised form, March 29, 2021 Published, Papers in Press, April 8, 2021,
https://doi.org/10.1016/j.jbc.2021.100639

Frank Oechslin*, Carmen Menzi, Philippe Moreillon, and Gregory Resch
From the Department of Fundamental Microbiology, University of Lausanne, Lausanne, Switzerland

Edited by Chris Whitfield

Endolysins are peptidoglycan hydrolases produced at the end of the bacteriophage (phage) replication cycle to lyse the host cell. Endolysins in Gram-positive phages come in a variety of multimodular forms that combine different catalytic and cell wall binding domains. However, the reason why phages adopt endolysins with such complex multidomain architecture is not well understood. In this study, we used the *Streptococcus dysgalactiae* phage endolysin PlySK1249 as a model to investigate the role of multidomain architecture in phage-induced bacterial lysis and lysis regulation. PlySK1249 consists of an amidase (Ami) domain that lyses bacterial cells, a nonbacteriolytic endopeptidase (CHAP) domain that acts as a dechaining enzyme, and a central LysM cell wall binding domain. We observed that the Ami and CHAP domains synergized for peptidoglycan digestion and bacteriolysis in the native enzyme or when expressed individually and reunified. The CHAP endopeptidase resolved complex polymers of stem-peptides to dimers and helped the Ami domain to digest peptidoglycan to completion. We also found that PlySK1249 was subject to proteolytic cleavage by host cell wall proteases both *in vitro* and after phage induction. Cleavage disconnected the different domains by hydrolyzing their linker regions, thus hindering their bacteriolytic cooperation and possibly modulating the lytic activity of the enzyme. PlySK1249 cleavage by cell-wall-associated proteases may represent another example of phage adaptation toward the use of existing bacterial regulation mechanism for their own advantage. In addition, understanding more thoroughly the multidomain interplay of PlySK1249 broadens our knowledge on the ideal architecture of therapeutic antibacterial endolysins.

Phage endolysins represent a fascinating family of peptidoglycan hydrolases that are critical for bacterial lysis and release of phage progeny at the end of the phage life cycle (1). They have gained recent interest in biomedical development as potential antibacterial agents (2–4). Phage endolysins target the bacterial peptidoglycan, an essential structure made of a complex meshwork of *N*-acetylglucosamine (GlcNAc)–*N*-acetylmuramic acid (MurNAc) glycan strands cross-linked by short stem peptides attached to MurNAc residues (5, 6). They can cleave various bonds between sugars or peptide chains and come in a variety of uni- or multimodular forms. Endolysins encoded by phages infecting Gram-positive bacteria are usually composed of several functional domains including glucosaminidases, amidases, and endopeptidases (referred to as catalytic domains or CDs) and cell-wall-binding domains (referred to as CBDs) (7–9).

In endolysins from Gram-positive bacteria, the architecture and functions of CDs and CBDs are quite variable. For instance, the well-characterized staphylococcal endolysins Lysk, Φ11, and MV-L, as well as streptococcal endolysins B30 and lambdaSa2 contain two CDs and one CBD (10–14). However, when individually tested in truncated constructs, only one of these CDs conferred bacterial lysis in a "lysis from without" scenario. For this reason, the functional role of nonbacteriolytic CDs is not entirely clear. It has also been hypothesized that their lytic activities were progressively lost through evolution and/or that they might be involved in reinforcing cell wall binding (15, 16).

CBDs are important to target the endolysin to its peptidoglycan substrate in addition to confer host specificity (17–20). They are commonly located at the N- or C-terminus of the protein and are rarely located in the central region (21, 22). However, CBDs are not always required for bacterial lysis since deleting them has even improved the lytic activity of some endolysins even without loss of specificity, as shown for endolysin B30, (7, 23, 24). Hence, nonbacteriolytic CDs or CBDs may have additional or alternative roles in the endolysin physiology.

In this work, we attempted to clarify the functional roles of the CDs and the CBD of the *Streptococcus dysgalactiae* phage endolysin PlySK1249 (25) and their implication in the physiology of phage-induced bacterial lysis. This endolysin has a complex structure with a central LysM CBD, an N-terminal amidase (Ami) domain, and a C-terminal Cysteine Histidine-dependent Amidohydrolase Peptidase (CHAP) domain. While amidases (or *N*-acetylmuramoyl-L-alanine amidases) are enzymes known to hydrolyze the amide bond between the *N*-acetylmuramoyl glycan moiety and the first L-ala of the

* For correspondence: Frank Oechslin, Frank.Oechslin@gmail.com.
Present address for Frank Oechslin: Department of Biochemistry, Microbiology and Bioinformatics, Université Laval, Quebec city, Canada.
Present address for Gregory Resch: Center for Research and Innovation in Clinical Pharmaceutical Sciences, Lausanne University Hospital, Lausanne, Switzerland.

© 2021 THE AUTHORS. Published by Elsevier Inc on behalf of American Society for Biochemistry and Molecular Biology. This is an open access article under the CC BY license (http://creativecommons.org/licenses/by/4.0/).

stem peptides (26), CHAP domains are primarily endopeptidases, sometimes with amidase activities (27).

We could observe that the Ami domain was a bacteriolytic amidase, whereas CHAP was a nonbacteriolytic endopeptidase that could synergize for efficient bacterial lysis. The CHAP domain also acted as a dechaining enzyme and shared high functional and structural analogies with dechaining autolysins present in lactococci or streptococci (28, 29). We finally notice that PlySK1249 was subject to proteolytic cleavage by cell wall proteases both *ex vivo* and after phage induction *in vivo*. Cleavage dismantled the CDs by hydrolyzing their linker regions, thus hindering their bacteriolytic cooperation and possibly modulating the lytic activity of the enzyme.

Like for proteolytic regulation of certain autolysins (30–32), PlySK1249 cleavage could represent a new mechanism of dual phage-bacterial regulation of endolysin-induced lysis. In addition, understanding more thoroughly the interdomain

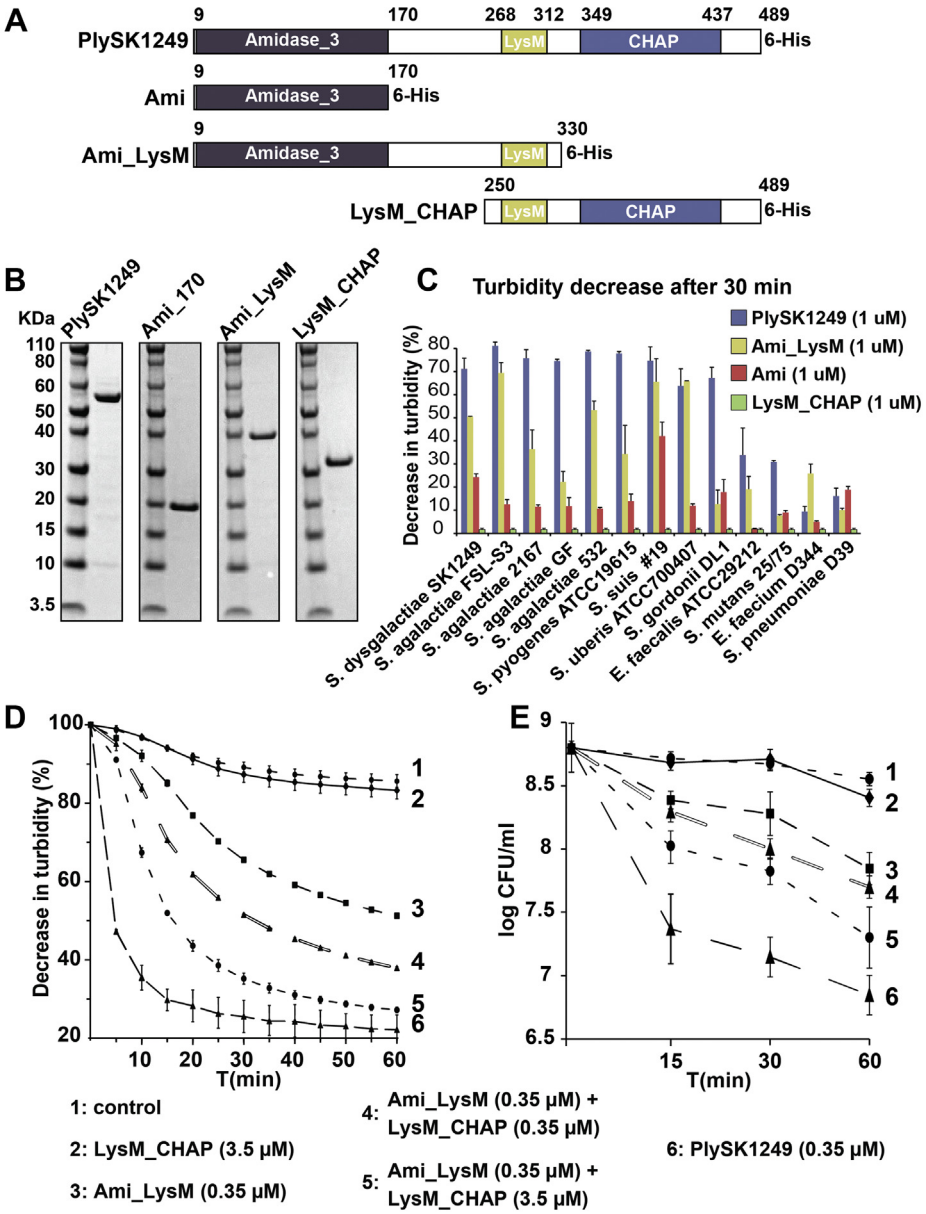

Figure 1. Characterization of the lytic activity of the PlySK1249 endolysin and its various truncated forms. *A*, parent PlySK1249 (full enzyme, aa 1–489); Ami (N-terminal amidase, aa 1–170); Ami_LysM (N-terminal amidase + LysM, aa 1–330); LysM_CHAP (LysM + C-terminal CHAP domain, aa 250–489). *B*, SDS-PAGE gel showing PlySK1249 and its various truncated constructions. The purified endolysin constructions were loaded (2 mg/ml) on NuPAGE 4 to 12% BisTris gels and stained with Coomassie blue. Molecular mass was determined with a prestained protein standard. *C*, cells of multiple bacterial species in the exponential growth phase were exposed to 1 µM of parent PlySK149 or its different truncated forms. Decrease in the turbidity of the cultures was measured at 600 nm after 30 min. No decrease in turbidity was observed in the absence of enzyme (not shown) or in the presence of LysM_CHAP. *D*, *S. dysgalactiae* cells in the exponential growth phase were also exposed to either 1 µM of Ami_LysM or LysM_CHAP constructs alone or in combination and the decrease in turbidity (at 600 nm) was followed over 1 h. *E*, viable counts from experiment shown in panel *D*. Counts were assessed by plating serial dilutions on nutrient agar. The experiments were repeated twice in triplicate and means ± standard deviations are shown.

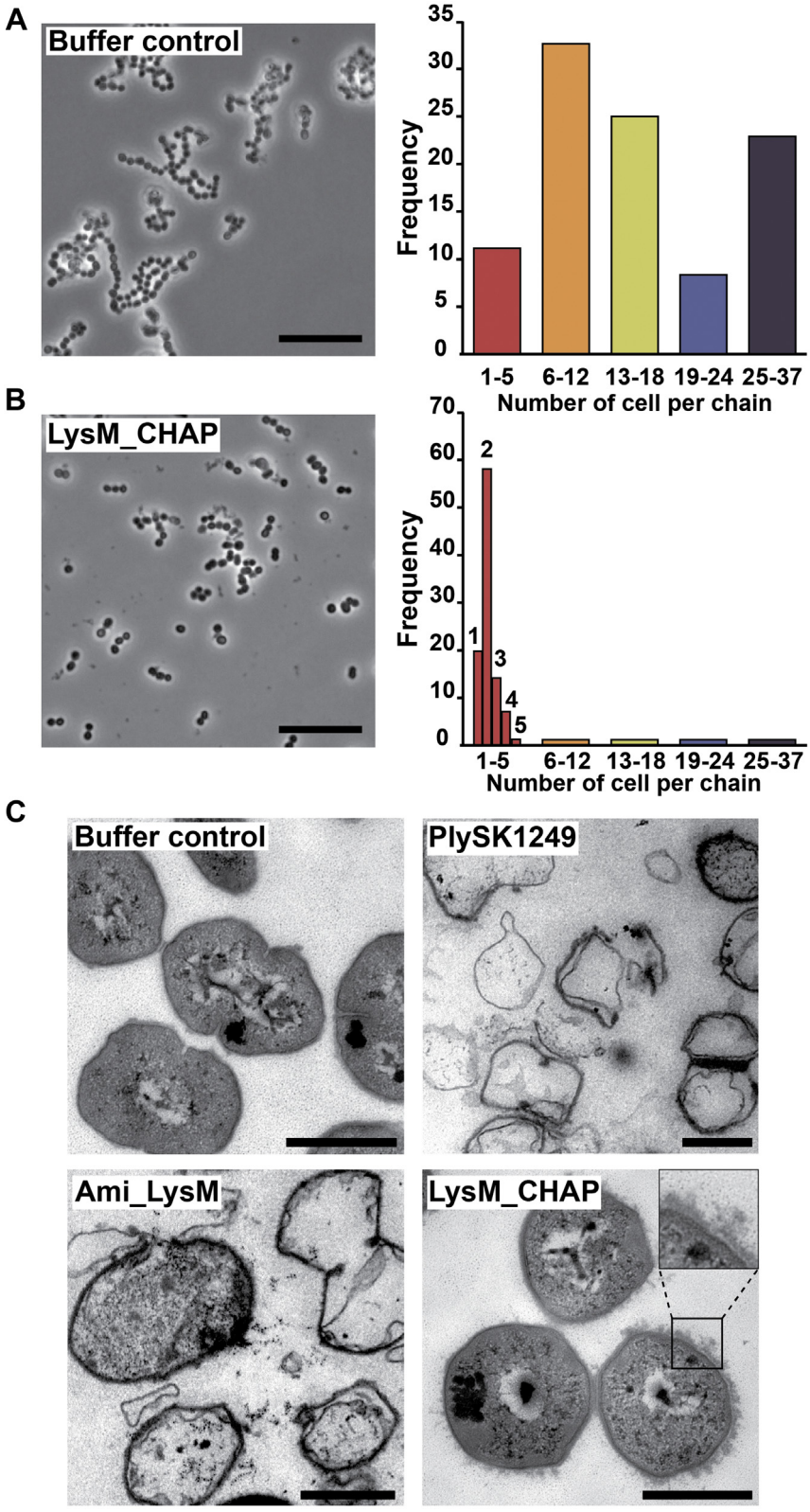

Figure 2. Morphological aspects of cells lysed by the PlySK1249 endolysin and its various truncated forms. *S. dysgalactiae* in the exponential growth phase were observed after 1 h using phosphate buffer as a control (*A*), or LysM_CHAP at a final concentration of 3.5 μM (*B*). Although the CHAP domain did not impact directly on cell lysis, an effect on chain disruption was observed. The control population was composed mainly (90%) of chains between 6 and 37 cells long (144 cells observed in total) compared to the 60% of chains that were composed of two cells for the LysM_CHAP treatment (1044 cells observed in total). *C*, transmission electron microscopy of *S. dysgalactiae* cells treated with the native PlySK1249 endolysin or its various truncated versions. *S. dysgalactiae* cells in the exponential growth phase were treated with phosphate buffer for 1 h as a control, Plysk1249 for 15 min, Ami_LysM for 15 min, or LysM_CHAP for 1 h. Cells were then postfixed using glutaraldehyde and embedded in epoxy for ultrathin sectioning. Scale bars represent 500 nm. The *inset* in the LysM_CHAP figure highlights the nonlytic wall nibbling by the LysM_CHAP construct.

interplay of PlySK1249 may be useful in the design of novel therapeutic lysins.

Results

Contribution and cooperation of each domain in the activity of the PlySK1249 endolysin

To assess the specific roles of each of the predicted domains, various truncated forms of PlySK1249 were generated (Fig. 1*A*). After being overexpressed in *Escherichia coli*, the protein constructs were purified by affinity chromatography using a 6xHis tag at the C-terminal position. The purity and the correct molecular weight were verified on 4 to 12% BisTris gels (Fig. 1*B*) (~54 kDa for PlySK1249, ~19 kDa for Ami, ~37 kDa for Ami_LysM, ~26 kDa for LysM_CHAP). Of note, the CHAP domain could not be overexpressed alone, it always required attachment to the LysM domain.

The relative contribution of the two CDs and the CBD to bacterial lysis was compared with the relative contribution of the parent enzyme. The constructs were first tested against an array of different Gram-positive bacteria (Fig. 1*C*). Parent PlySK1249 was more lytic against *Streptococcus* spp. than against more distantly related species, such as enterococci. Moreover, and apart from a few exceptions, the PlySK1249 truncated forms were less active than the parent enzyme, with Ami_LysM being generally more active than Ami alone and LysM_CHAP showing no lytic activity even when incubated for 2 h (Fig. 1*C* and data not shown).

We further tested the possibility of a cooperative activity between the Ami and CHAP catalytic domains by following the loss of turbidity and cell viability when used alone or mixed together against *S. dysgalactiae* 1249 cells (Fig. 1, *D* and *E*, respectively). The results confirmed the decrease of intrinsic lytic activity of the subdomains observed in Figure 1*C* (Fig. 1*D*). Indeed, while PlySK1249 caused a rapid 50% drop in turbidity within 5 min, Ami_LysM showed intermediate lysis (50% drop in turbidity in 1 h) and LysM_CHAP was not lytic at all. However, adding equimolar amounts of nonlytic LysM_CHAP to Ami_LysM gradually increased lysis while a 1/10 Ami_LysM/LysM_CHAP ratio almost completely restoring lysis efficiency at 1 h, as compared with the parent PlySK1249. This interdomain cooperation was formally synergistic (*i.e.*, the effect of the domain combination was superior than the sum of their individual effects) and was also observed between Ami and LysM_CHAP (data not presented). These results correlated with the viable cell counts obtained in time-kill assays (Fig. 1*E*).

The nonlytic LysM_CHAP construct has an intrinsic dechaining activity

A closer look at the LysM_CHAP activity using optical and Transmission Electron Microscopy (TEM) revealed subtle nonlytic effects (Fig. 2). Phase-contrast optical microscopy of exponential phase cultures (OD_{600nm} 0.5) of *S. dysgalactiae* SK1249 showed that they were composed of 90% of chains ranging from 6 to 37 cells (Fig. 2*A*). However, 1 h of incubation with LysM_CHAP resulted in chain disruption with the majority (60%) of chains harboring only 1 to 5 bacteria, the rest of them being distributed over longer structures (Fig. 2*B*).

This nonlytic activity was further supported by TEM imaging. Control cells incubated in PBS alone showed a typical Gram-positive bacterial shape (Fig. 2*C*, Buffer control). Cells treated with PlySK1249 or Ami_LysM were lysed as assessed by the presence of a majority of ghost cells (15 min incubation, Fig. 2*C*, PlySK1249 and Ami_LysM). Treatment with LysM_CHAP alone resulted in round swelling cells with surface alterations but absence of lysis even after 1 h exposure (Fig. 2*C*, LysM_CHAP).

The N-terminal Ami domain of PlySK1249 is an amidase while the C-terminal CHAP domain is an endopeptidase

To better understand the contribution of each CD domains to the overall activity of the enzyme, we further looked at their specific peptidoglycan cleavage sites. Glycosidase or peptidase activity was first assed for PlySK1249 and its truncated constructs using purified *S. dysgalactiae* cell wall. Compared with the N-acetylmuramidase mutanolysin, none of the constructs had glycosidase activities according to Park–Johnson assay (Table S2). In contrast, using a modified Ghuysen assay, free amino groups release was measured after peptidoglycan hydrolysis by PlyKS1249 and all the PlySK1249-derived constructs, therefore identifying an amidase and/or endopeptidase activity.

To discriminate between amidase and endopeptidase activities for the Ami and CHAP catalytic domains, digested peptidoglycan was further analyzed RP-HPLC and LC-MS for the presence of precursor masses containing the stem peptide motif AQKAAA and polymers of it. After digestion with PlySK1249, two major peaks with relatively short retention times were identified by RP-HPLC (at approximately 35 and 42 min, Fig. 3*A*.I). These were mainly identified as stem peptides dimers by LC-MS, also presence of monomers and trimers was detected (Fig. 3*B*). After digestion with Ami_LysM or Ami alone, the two major peaks became marginal and were replaced by an array of smaller peaks eluting later in the RP-HPLC profile (between 55 and 90 min, Fig. 3*A*.II and Fig. S1*A*, respectively). LC-MS analysis showed that these peaks covered an array from trimers to heptamers that eluted later in RP-HPLC profiles (Fig. 3*B* and Figs. S2 and S3). Moreover, identical profiles were obtained for Ami and Ami_LysM, indicating that the LysM CBD was not responsible for altering the hydrolytic profile (Fig. S1*A*).

The digestion with LysM_CHAP did not yield any major peak pattern, although two small peaks could be observed at 36 and 42 min. These peaks were not observed with the Ami domain alone but were present in the PlySK1249 digestion (Fig. S1, *B* and *C*). This indicates that the LysM_CHAP construct is able to solubilize peptidoglycan to a very small extend, which can be attributed to its endopeptidase activity. Indeed, internal hydrolysis of the peptide cross bridges does not disconnect stem peptides from the glycan fraction, which is lost during the sequential glycan precipitation. Importantly,

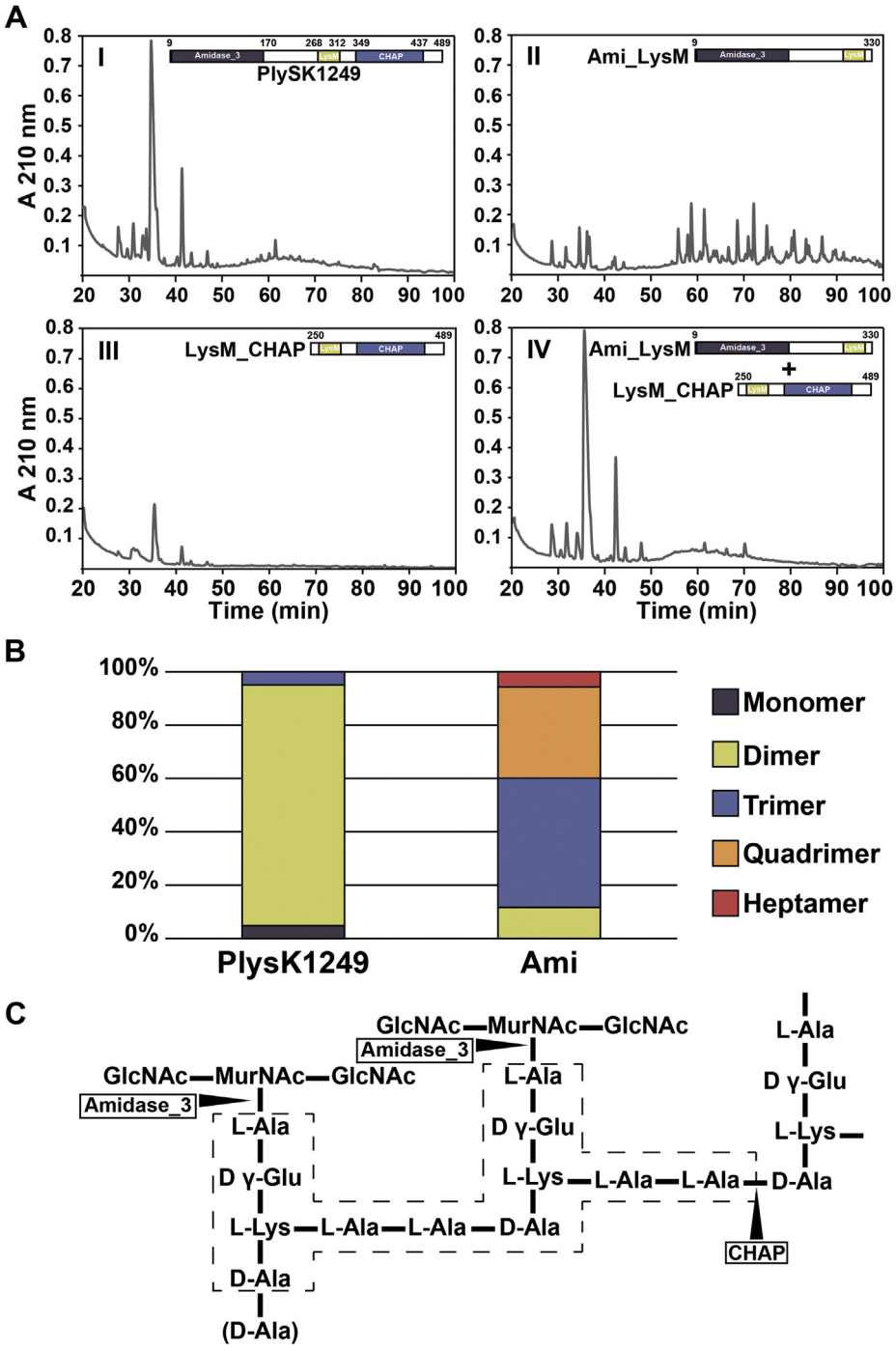

Figure 3. RP-HPLC chromatogram and LC-MS analysis of *S. dysgalactiae* peptidoglycan digested with PlySK1249 or its truncated catalytic domains. *A*, purified wall-peptidoglycan was digested overnight and glycans were sequentially precipitated before chromatography on a C18 Sephasil column. Equimolar concentrations (3.5 μM) of I) PlySK1249, II) Ami_LysM, III) LysM_CHAP, and IV) both Ami_LysM and LysM_CHAP were used and analyses were repeated three times for each, yielding the same results. *B*, relative abundances of the polymers observed in the native enzyme and amidase domain digestion experiments. The products of peptidoglycan digestion by the native enzyme and its truncated Ami domain were analyzed by LC-MS after a 5 kDa filtration. The masses of the precursors corresponding to the dimer, trimer, quadrimer, and heptamer of the AAAQKA monomer block were detected. All of these oligomers were detected in both samples, with the exception of the heptamers, which were only present in the amidase digestion. Polymer structures were deduced from masses after *de novo* peptide sequencing. *C*, representation of *S. dysgalactiae* peptidoglycan based on the masses and sequences observed. *Arrows* indicate the cleavage sites for the respective catalytic domains of the enzyme. The framed *dotted-line* area corresponds to the dimer block.

combining LysM_CHAP with Ami_LysM restored the complete digestion pattern of the whole PlySK1249 enzyme (Fig. 3*A*.IV). The fact that the digestion product of the native enzyme is mainly composed of dimers also indicates that LysM_CHAP could resolve stem-peptide multimers mainly to dimers, but rarely to monomers. Since glycan strands can remain connected through dimer crosslinks, which are sufficient to maintain a loose polymer structure and thus prevent

bacterial lysis, this might explain why the CHAP domain is not directly lytic on its own. Finally, the digestion products summarized in Fig. S2 confirmed an N-acetylmuramoyl-L-alanine activity for the Ami domain and most probably an L-Ala-D-Ala endopeptidase activity for the CHAP domain according to the predicted structure of the dimer (Fig. 3*C*).

PlySK1249 is composed of proteolytic-resistant core domains connected by proteolytic-susceptible linkers

The complex nature of PlySK1249 may be a source of instability as previous authors observed degradation of multi-domain autolysins by cell-wall-associated proteases (30–32). For this reason, we tested the resistance of PlySK1249 to protease-induced cleavage first by trypsin and second by bacterial-wall-associated proteases.

Proteolytic cleavage of PlySK1249 was observed to be restricted to the two linkers connecting the different enzyme active domains, while the active domains themselves were left intact. Two bands having a lower molecular mass could be observed after overnight incubation of the endolysin with 1 μg/ml of trypsin (Fig. 4*A*). Amino acid sequencing of extracted bands confirmed the presence of two peptides corresponding to the CHAP (aa 318–489) and Ami (aa 1–204) CD domains in the upper band 1 and the Ami (aa 1–175) domain only in the lower band 2 (Table S3). These results were also confirmed by western blotting using Anti-6xHis tag antibodies. Similar results were finally observed when the Ami_LysM or the LysM_CHAP constructs were exposed to trypsin degradation, which also resulted with the cleavage of the connecting linkers (Fig. 4, *B* and *C*). Thus, PlySK1249 was composed of different trypsin-resistant cores corresponding to the CD and CBD domains and trypsin-susceptible linker regions.

Extracts of *S. dysgalactiae* SK1249 cell-wall-associated proteins were also prepared and incubated with either the native enzyme or the Ami_LysM and LysM_CHAP constructs (Fig. 4*D*). Due to the large number of proteins in the cell wall extract, it was not possible to visualize the degradation products by Coomassie-blue staining. Therefore, western blotting with an Anti-6xHis tag antibody was used

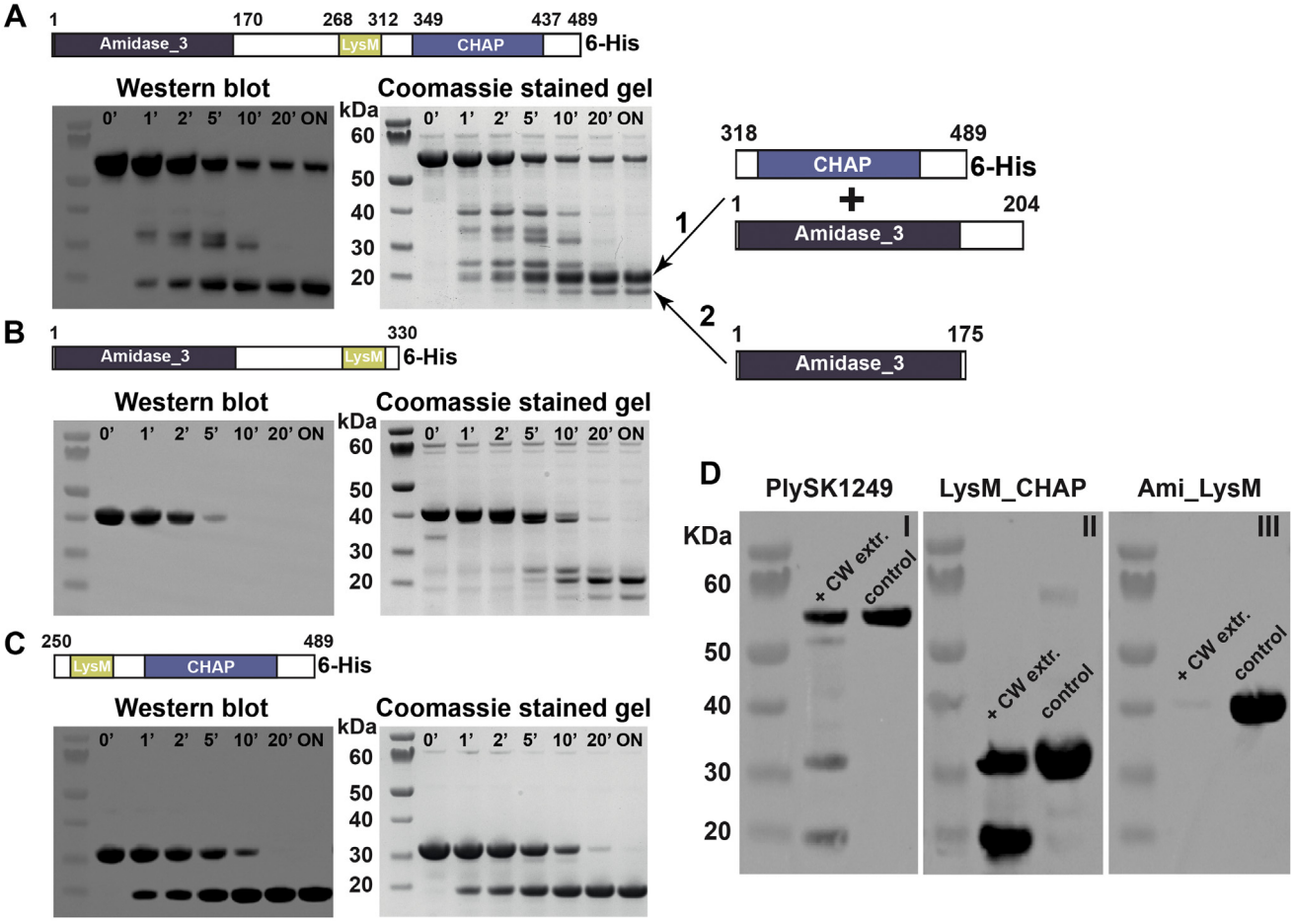

Figure 4. PlySK1259 proteolysis and its different truncated versions in the presence of trypsin or cell-wall-associated proteases. Forty μM of the parent enzyme (*A*) or the Ami_lysM (*B*) and LysM_CHAP (*C*) were incubated with 1 μg/ml of trypsin. *Right panels*, sample were migrated after different incubation times on NuPAGE 4 to 12% BisTris, stained with Coomassie blue. The subsequent degradation products obtained after ON digestion of the native enzyme (band 1 and 2) were sequenced and the identified peptides are indicated on the *right of the panel*. *Left panels*, digestion products were transferred to a nitrocellulose membrane for western blotting using Anti-6xHis antibody. *D*, 40 μM of the parent enzyme (I), Ami_lysM (II), or LysM_CHAP (III) were incubated overnight with cell wall protein extract from *S. dysgalactiae* SK1249. Samples were migrated on NuPAGE 4 to 12% BisTris and degradation was confirmed by western blotting using Anti-6xHis tag antibody.

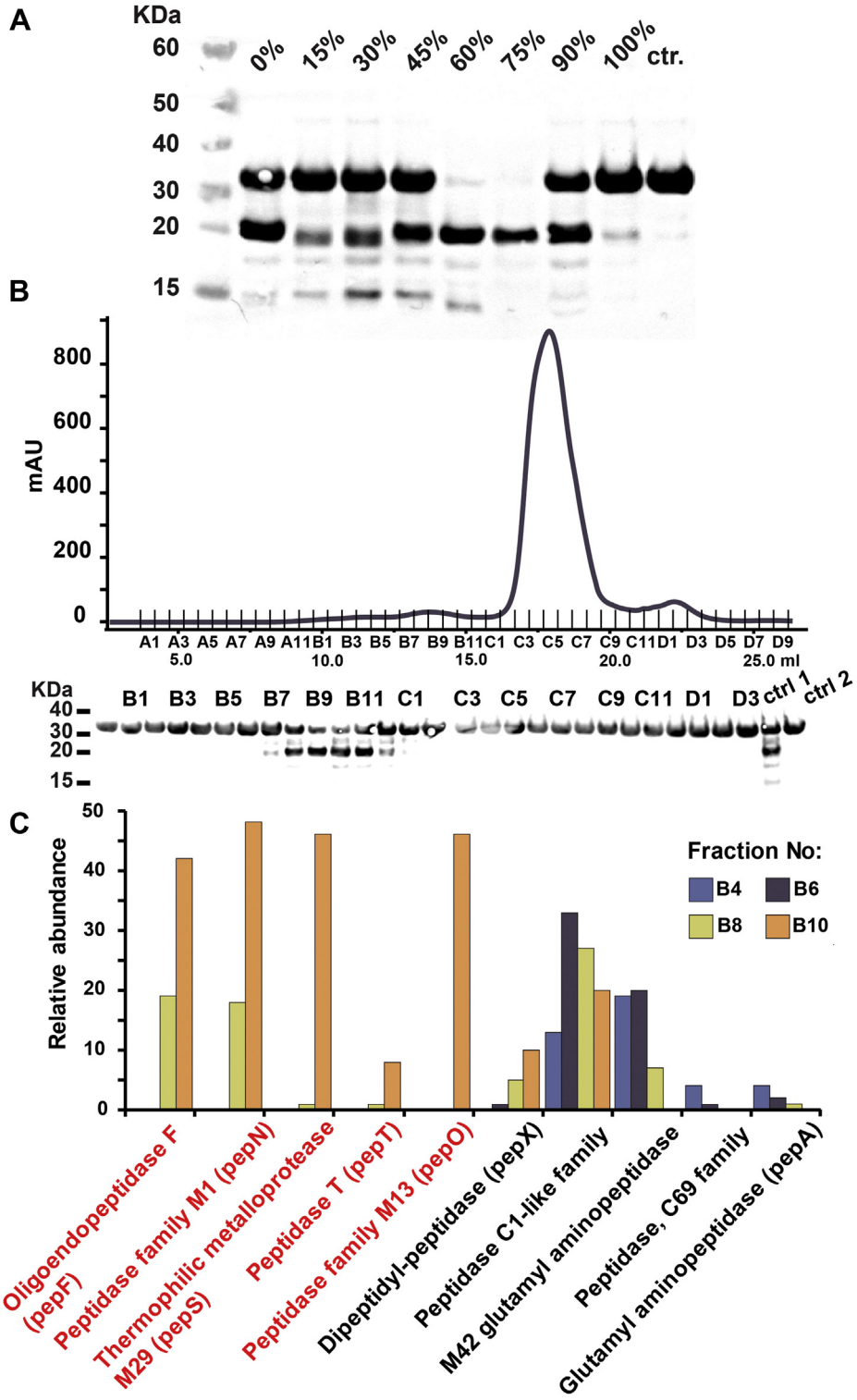

Figure 5. Identification of the proteases involved in the PlySK1249 cleavage. *A*, proteins present in the total cell wall extract were serially precipitated using increasing concentrations of ammonium sulfate. Between each step, proteins were collected by centrifugation and then mixed with 40 μM of the LysM_CHAP construct and incubated overnight. Samples were then migrated on a NuPAGE 4 to 12% BisTris gel and degradation was confirmed by western blotting using Anti-6xHis tag antibody. *B*, the 55% to 80% ammonium sulfate precipitation fraction was further separated using size-exclusion chromatography. Fractions were tested for activity as described before. *C*, relative abundances after LC-MS analysis of the protease content present in the fractions B4, B6, B8, and B10. Proteases only observed in the active fractions B8 and B10 are highlighted in *red* (pepF, N, O, S, T).

as for trypsin digestion. After overnight incubation, two bands were generated for PlySK1249 at approximately 30 and 20 kDa, which were absent in the control with the endolysin alone, as well as in the wall protein extract (result not shown) (Fig. 4*D*.I). Degradation was also observed for the LysM-CHAP construct with an additional band at 20 kDa

(Fig. 4*D*.II). Due to the position of the 6xHis tag in the C-terminal part of the enzyme, the Ami domain alone was not observed (Fig. 4*D*.III). Importantly, these results are similar to the one observed using trypsin and confirmed that PlySK1249 was cleaved between its two linkers, by both trypsin and cell-wall proteases.

Insights into the nature of the wall proteases

We used a bioactivity-guided fractionation protocol to identify the host cell-wall-associated proteases that are responsible for PlySK1249 degradation (Fig. 5). Ammonium sulfate was used for a first round of sorting and fractions were tested on the LysM_CHAP construct. LysM_CHAP proteolytic degradation was observed for fractions precipitated at 60% to 75% sulfate ammonium (Fig. 5*A*). A second purification step was performed by size-exclusion chromatography using a 55% to 80% ammonium sulfate fraction, and the output was again tested for proteolytic activity on the LysM_CHAP construct (Fig. 5*B*). Four different fractions (B4, B6, B8, and B10) were further analyzed by LC-MS and a total of ten different host-associated proteases could be detected (Fig. 5*C*, Table S4, and Supplemental Data 1). Five of them (namely pepF, pepN, pepO, pepS, pepT) were observed only in the two proteolytic active fractions B8 and B10, which indicate that PlySK1249 can be cleaved by a specific subset of host associated proteases.

Endolysin cleavage also occurred during in vivo *prophage induction*

As a proof of concept, we further tested whether endolysin-specific cleavage products could also be generated during phage induction *in vivo*. Unfortunately, we could not induce the prophage carrying PlySK1249 from its natural *Streptococcus dysgaactiae* host. Therefore, we took advantage of *Streptococcus agalactiae* strain FSL S3-026, for which full genome is available (https://www.ncbi.nlm.nih.gov/nuccore/AEXT00000000.1) and which contains a single LambdaSa04-like prophage that is inducible with mitomycin C. This prophage carries an endolysin closely related to PlySK1249 (further named PlySK1249*; see Experimental procedures section and Fig. S4*A*), including the same domain architecture and 80% aa homology with the PlySK1249 endolysin (Fig. S4*B*).

Cultures of *S. agalactiae* FSL-S3 were either induced with mitomycin C or left uninduced as negative controls (Fig. 6*A*). Supernatants were then collected after 6 h and loaded on an SDS-PAGE gel (Fig. 6*B*). The gel was split into five different fragments covering a range of molecular weights from 75 to 10 kDa and further analyzed by LC-MS for the presence of prophage proteins. A total of 11 prophage-related proteins were identified in the supernatant of the induced culture and, to a much lesser extent, in the noninduced fractions, suggesting basal induction of the prophage (Table S5 and

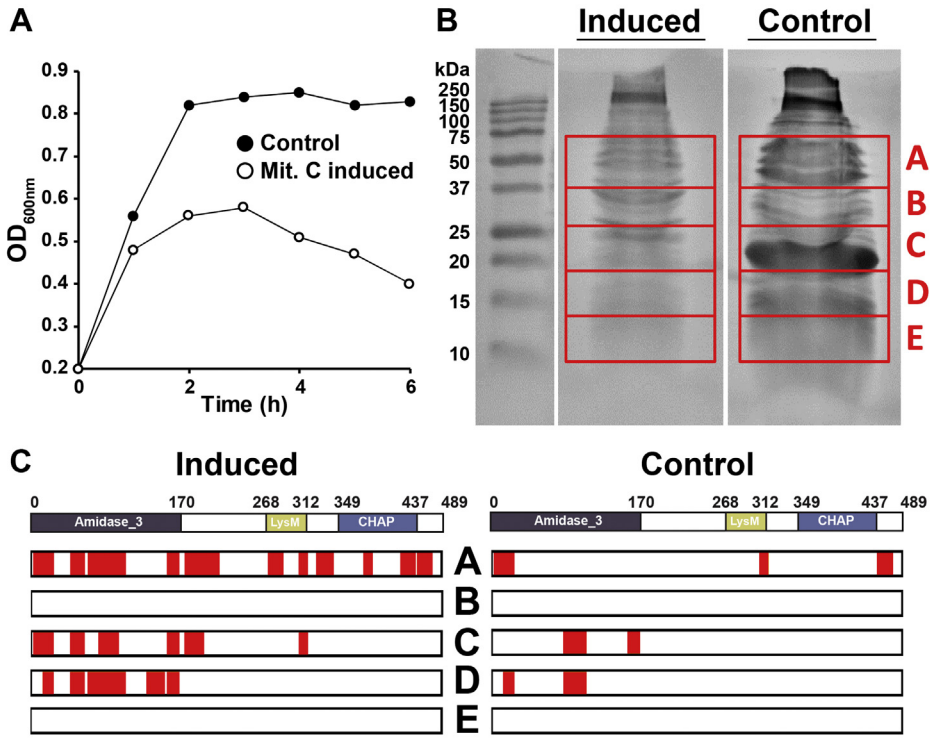

Figure 6. PlySK1249-like endolysin proteolysis *in vivo* during prophage induction in strain *S. agalactiae* FSL-S3. *A*, the LambdaSa04-like prophage inserted in the *S. agalactiae* FSL-S3 strain was induced by adding 1 μg/ml of mitomycin at an OD_{600nm} of 0.2 and lysis of the culture was followed for 6 h (full circle noninduced, empty circle mitomycin C-induced culture). *B*, the supernatant of the culture was then concentrated 5000× time and migrated onto a 15% SDS gel. A total of five bands were cut from the gel, covering a molecular weight range of 75 to 10 kDa. *C*, extracted bands from the gel were analyzed by LC-MS for the presence of the PlySK1249-like endolysin in both induced and uninduced cultures. Peptides detected that matched with the PlySK1249-like amino acid sequences are highlighted in *red*.

Supplemental Data 2). A closer look at the peptides that were detected in the different gel fragments indicated that PlySK1249* was present in the supernatant in its original form, but also in specific cleavage products (Fig. 6*C*). Peptides covering the total lengths of the enzyme were detected in band A (ranging from approximately 75–40 kDa) mainly in induced

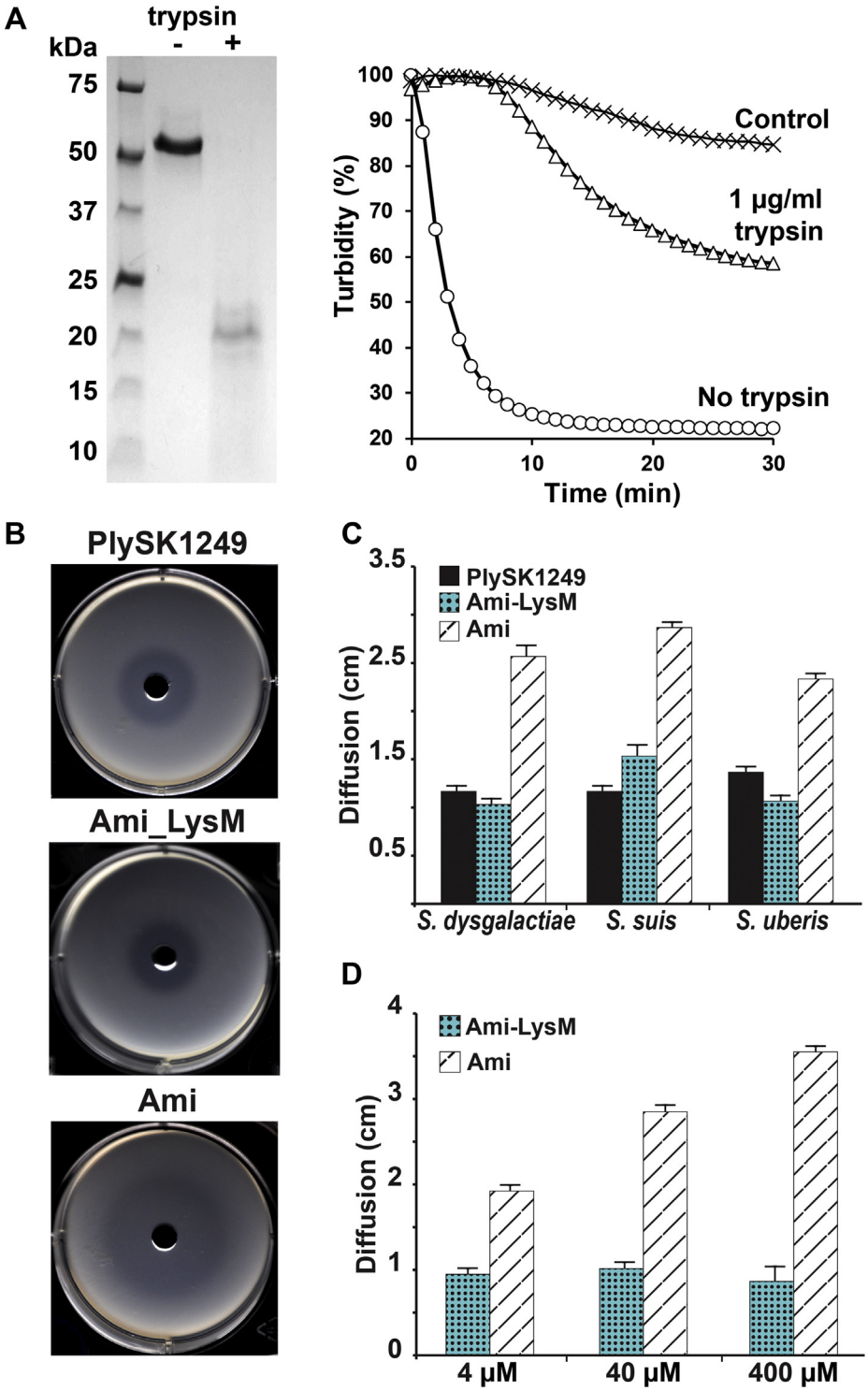

Figure 7. Effect of proteolytic cleavage on PlySK1249 lytic activity and impact of endolysin truncation on diffusion. *A*, *S. dysgalactiae* cells in the exponential growth phase were exposed to 3.5 µM of PlySK1249 or 3.5 µM of PlySK1249 pretreated with 1 µg/ml of trypsin during 30 min. Decrease in bacterial cell turbidity was measured at 600 nm during 30 min. *B*, PlySK1249, Ami, and Ami_LysM (40 µM) diffusion across a layer of soft agar containing heat-inactivated *S. dysgalactiae* cells with formation of a lysis halo. *C* and *D*, diffusion of the amidase domain was compared with the Ami_LysM construct and the native enzyme at a concentration of 40 µM and on different streptococcal species (*C*) or at different concentrations for the Ami and Ami_LysM constructs (*D*). Each experiment was repeated three times. Means ± standard deviations are shown.

cultures and somewhat in noninduced samples. Peptides covering the Ami_LysM and Ami catalytic sites were also observed in the lower part of the gel at two different positions, indicating cleavage in the linkers on both sides of LysM. This fulfilled the concept that linker-domain-specific cleavage of PlySK1249* endolysin did occur *in vivo* as observed with its PlySK1249 homologue *in vitro*. Finally, specific degradation was also confirmed when compared with the degradation patterns of the other phage proteins, for which only unspecific degradation was observed (Fig. S5). These results further support the specificity of the endolysin cleavage sites.

Possible implication of proteolytic cleavage for endolysin activity

The effect of proteolytic cleavage on the activity and diffusion of PlySK1249 was finally investigated (Fig. 7). Incubation of PlySK1249 with trypsin for half an hour resulted in a reduced lytic activity on *S. dysgalactiae* SK1249 cells. Indeed, a turbidity decrease of only 40% was observed after 30 min compared with an 80% decrease after 10 min without trypsin (Fig. 7*A*).

Because proteolytic cleavage also resulted in the separation of the LysM-binding domain from the catalytic sites, we measured the diffusion of PlySK1249, Ami, and Ami_LysM across a layer of soft agar containing heat-inactivated *S. dysgalactiae* SK1249 cells. Due to the lytic activity of the amidase domain, we evaluated the diffusion of the different constructs by measuring the diameters of the clear halos produced by bacterial lysis (Fig. 7*B*). LysM prevented diffusion of the Ami domain when tested against three different streptococci (average diameter decreased from ∼2.5 cm for Ami compared with ∼1 cm for Ami_LysM, Fig. 7, *D* and *E*). The diffusion of PlySK1249 was similar to that of Ami_LysM, indicating that the phenomenon was independent of the protein molecular weight (Fig. 7, *D* and *E*). In addition, diffusion of Ami was concentration-dependent, whereas LysM prevented diffusion over a >100-fold range of concentrations (Fig. 7*F*).

Discussion

In the present study, we aimed at understanding the individual and cooperative roles of the PlySK1249 functional domains, as well as their potential involvement in endolysin lysis regulation. Using the parent enzyme and truncated constructs, we found that the three domains cooperated to increase the overall lytic activity of the enzyme. Although CHAP was not bacteriolytic, it did have a substantial cooperative effect (which was in fact synergistic since the activity of combined domains was greater than the sum of the activities of individual domains) when combined with Ami as in the context of native PlySK1249.

We further investigated the functions of the three domains and demonstrated that the nonbacteriolytic CHAP domain had a dechaining activity that also contributed to peptidoglycan solubilization. CHAP was an L-Ala-D-Ala endopeptidase that resolved complex polymers of stem-peptides to dimers and helped the Ami domain to digest peptidoglycan to completion. Moreover, resolving polymers to dimers rather than to monomers explained the lack of CHAP bacteriolytic activity, as dimeric stem-peptides could keep glycan chains cross-linked and ensure a minimal cell wall skeleton. In contrast, complete digestion to monomers would have let the network of glycan chains fall apart, which should have resulted in bacteriolysis.

The CHAP dechaining activity is reminiscent of cell wall maturation by autolysins in *Bacillus subtilis*, which also act as dechaining enzymes, as well as the Cse autolysin of *Streptococcus thermophilus*, which is composed of a LysM and a CHAP domain that promotes cell separation (28, 29). Not unexpectedly, functionally common domains may serve different purposes in different backgrounds. While functional dissection of endolysin subdomains has been reported before, delving into the enzymatic contribution of each individual subdomains helped to reconcile the synergistic contribution of the nonbacteriolytic CHAP to the overall endolysin activity and wall solubilization. Although silent in terms of cell lysis, the CHAP domain is a genuine endopeptidase actively complementing the Ami domain.

This intramolecular domain cooperation could be modulated by the action of host cell-wall-associated proteases. We could observe specific proteolytic cleavage taking place in the linkers connecting both CDs to the central LysM CBD when PlySK1249 was coincubated with cell-wall-associated proteases or during cell lysis by prophage induction. A subset of five different metalloproteases could be identified as potential candidate. This includes three aminopeptidases (pepN, pepS, and pepT) and two endopeptidases (pepO and pepF) (33), the latter two are more likely to be directly involved in the proteolytic cleavage since it is taking place inside the protein. This potential regulatory mechanism could serve the purpose of dismantling domain proximity—and domain cooperation—therefore modulating the lytic activity of the enzyme. A similar phenomenon was previously observed for the main autolysins AtlA of *Enterococcus faecalis* and AcmA of *Lactococcus lactis*, which were also degraded by cell wall proteases (30–32). In the case of AcmA, proteolytic cleavage resulted in a reduced enzymatic and cell wall binding activity (30, 31, 34).

In summary, the presented observations provide a rationale for the multimodular architecture of PlySK1249, which could possibly be extended to other multimodular lysins. While both catalytic domains were observed to act coordinately to optimize bacterial lysis, the CBD is expected to delay diffusion until proteolytic inactivation of the lysin by host cell-wall-associated peptidases is completed. This could also possibly protect neighboring bacteria and sibling prophages from deleterious lysis. Moreover, the multimodular structure of PlySK1249 might provide a way to channel several functions in a single protein as subsequent protein cleavage or maturation would free the modules to perform different functions, *i.e.*, Ami for lysis and CHAP for dechaining.

These observations have both theoretical and practical implications. From the theoretical point of view, it raises the question of coevolution between endolysin/autolysin and host bacteria. Endolysins and autolysins are likely to have common

ASBMB

ancestors, and bacteria can regulate the activity of autolysins posttranslationally (*i.e.*, in the peptidoglycan) for the purpose of cell wall maturation. It now appears that the phage endolysin studied herein undergoes similar bacterial-dependent posttranslational modification, highlighting the possible adaptation of phage endolysins toward the use of existing bacterial regulation mechanism for their own advantage.

From the practical point of view, it opens new perspectives on the ideal architecture of therapeutic antibacterial endolysins. Indeed, this is particularly relevant for the design of new chimeric endolysin, where domains that do not show lytic activity should not be necessarily dismissed. Indeed, when combined with appropriate partners, they could enhance the lytic properties of other CD domains. Moreover, the implication of the linkers should not be underestimated and further investigated in regard to enzyme stability during therapeutic use.

Experimental procedures

Cell culture and growth conditions

All bacterial strains used in this study are listed. Gram-positive bacteria were grown at 37 °C in Brain Heart Infusion (BHI, Becton Dickinson) broth and plated on Mueller Hinton agar with 5% sheep blood (bioMérieux SA). Broth cultures of streptococci and enterococci were grown without aeration. *E. coli* were cultured at 37 °C in Lysogeny Broth (LB) with agitation (220 rpm) or plated on LB Agar (LA). The following compounds (at final concentrations) were added to the media when necessary: kanamycin sulfate (30 μg/ml), chloramphenicol (25 μg/ml for LA plates and 50 μg/ml for LB) or isopropyl β-D-1-thiogalactopyranoside (IPTG) (0.4 mM). Culture stocks were prepared from cells in the exponential growth phase in 20% glycerol (vol/vol) and stored at −80 °C. All chemicals were reagent-grade, commercially available products.

Cloning, expression, and purification of the truncated versions of the PlySK1249 enzyme

The plasmid pPlySK1249^{28a} (25) was used as a template for PCR amplification of genes encoding for truncated forms of the PlySK1249 endolysin (Fig. 1*A*) using specific primer pairs listed (Microsynth AG). PCR products were digested using restriction enzymes NcoI and XhoI (Promega) and ligated into predigested expression vector pET28a. Obtained plasmids (namely pAmi^{28a}, pAmi_LysM^{28a}, and pLysM_CHAP^{28a}, Table S1) were transformed in One Shot BL21 (DE3) pLysS chemically competent *E. coli* cells (Life Technologies Europe B.V.). Plasmid DNA was purified using the Qiagen Miniprep kit following the manufacturer's recommendations and all constructs were validated by DNA sequencing using universal T7 primers (Table S1). Following 0.4 mM IPTG induction for 18 h, recombinant proteins were purified by affinity chromatography as described previously (25) and loaded on NuPAGE 4 to 12% BisTris gels (Invitrogen) to confirm the correct molecular weights and assess their purity.

Evaluation of the antibacterial efficacy of lysins

Efficacy of bacterial lysis was measured for the parent PlySK1249 endolysin and its various truncated constructs by following the decrease in OD_{600nm} of a bacterial suspension as previously described (25). In order to assess the potential interaction between Ami_LysM or Ami and LysM_CHAP, the truncated enzymes were mixed together at different molar ratios ranging from 1:1 to 1:10. *In vitro* time-kill assays were performed as described elsewhere (25).

Light and electron microscopy

S. dysgalactiae cells were incubated with the various endolysin constructs at a concentration of 3.5 μM for 15 min for the PlySK1249 and Ami_LysM constructs and for 1 h for the control and the CHAP domain. For light microscopy, cells were immobilized on 1% agarose pads and phase-contrast microscopy images were taken with a Plan-Apochromat 100X/1.45 oil Ph3 objective on an AxioImager M1 microscope (Zeiss). For TEM, cell suspensions were treated with glutaraldehyde (25% final concentration) for 1 h at room temperature (RT) and washed with phosphate-buffered saline (PBS). The same procedure was applied for metaperiodate (1% final concentration, 15 min incubation at RT) and osmium tetroxide plus hexacyanoferrate (1% and 1.5%, respectively, 1 h incubation at RT). Cells were then centrifuged and the pellets were spun down in microcentrifuge tubes containing melted agar. After solidification of the agar, pellets were embedded in epon for ultrathin sections that were prepared as described by Broskey *et al.* (35). Micrographs were taken with a TEM FEI CM100 (FEI) at an acceleration voltage of 80 kV with a TVIPS TemCam-F416 digital camera (TVIPS GmbH).

Purification and digestion of peptidoglycan

Peptidoglycan of *S. dysgalactiae* SK1249 was purified as previously described (36). Briefly, 10 ml of an overnight culture was added to 1 l of fresh BHI medium. The cells were grown until an OD_{600nm} of 0.4 to 0.5 and then quickly cooled in an ice bath for 5 to 10 min. The culture was centrifuged at 4 °C and resuspended in PBS to reach a total volume of 40 ml. The bacterial suspension was poured dropwise into 40 ml of boiling sodium dodecyl sulfate (SDS) (8%) and boiled with agitation for 15 min to inactivate intrinsic autolytic enzymes. The cells were centrifuged at 20 °C to avoid SDS precipitation, washed twice with NaCl 1 M and five times with dH_2O. After the final washing step, the bacterial pellet was resuspended in 2 ml dH_2O and stored at −20 °C overnight. The following day, the cells were broken using a FastPrep homogenizer (Thermo Savant FastPrep FP120 Homogenizer) during three bursts of 45 s at 6.5 m/s with a 5 min cooling step between each burst. The supernatant was transferred into a tube and centrifuged at 13,000 rpm for 5 min at 4 °C and then again for 20 min at 4 °C. The pellet was resuspended in 3 ml Tris (0.1 M), 0.3 ml NaN_3 (0.5%), pH 7.5. After the addition of 0.3 ml $MgSO_4$ (200 mM), 60 μl DNAse (0.5 mg/ml), and 60 μl RNase (2.5 mg/ml), the mixture was incubated for 2 h at 37 °C with agitation, and then

overnight after 0.3 ml $CaCl_2$ (100 mM) and 0.3 ml trypsin (100 μg/ml) were added. For the final steps, SDS (1% final concentration) was added to the preparation, which was then heated for 15 min at 75 °C to extract digested peptides. After an additional centrifugation for 20 min at 20 °C and 13,000 rpm, the pellet was washed once with dH_2O, resuspended in 20 ml LiCl (8 M) and incubated at 37 °C with agitation for 15 min. The mixture was again centrifuged at 13,000 rpm, 4 °C for 20 min. Pellet was resuspended in 20 ml EDTA (0.1 M) to remove material bound by ionic interactions. Lastly, the bacterial peptidoglycan was centrifuged, washed twice with 2 ml dH_2O, and resuspended in 2 ml dH_2O. Aliquots of 1 ml were transferred into preweighed Eppendorf tubes and dried overnight by rotary evaporation (UniEquip UNIVAPO 150 ECH). The dried bacterial peptidoglycan was then resuspended to reach a concentration of 10 mg/ml. For enzymatic digestion, 100 μl of the extracted peptidoglycan was mixed with 900 μl of the previously purified endolysin constructs at 3.5 μM. The mixture was incubated overnight at 37 °C with agitation. The following day, the solution was heated for 3 min at 100 °C to inactivate the endolysin, then centrifuged at 13,000 rpm, RT for 10 min, and the supernatant containing the solubilized walls was transferred into a new tube.

Biochemical analysis of PlySK1249 hydrolysis sites in the peptidoglycan

Peptidoglycan extraction was performed as described above. Reducing sugar analysis was conducted using a modified Park–Johnson assay, and free amino acids were quantified with a modified Ghuysen procedure with 1-fluoro-2.4-dinitrobenzene, as described by Schmelcher *et al.* (37). Undigested peptidoglycan was used as a blank and glucose or L-Alanine calibration curves were used for calculations. All experiments were performed in triplicate.

Analysis of the digested peptidoglycan using reverse phase–high-pressure liquid chromatography (RP-HPLC)

The digested peptidoglycan was kept at −80 °C for 5 min and then dried overnight by rotary evaporation. After the addition of 0.5 ml of acetone, the tube was sonicated to resuspend the pellet, and another 1 ml of acetone was added to remove any contaminating endotoxins. The tube was left at RT for 30 min and then centrifuged at 13,000 rpm, RT for 10 min. The supernatant was dried by rotary evaporation for 10 min. In total, 200 μl dH_2O was added before sonication. Samples was stored at −80 °C for 5 min and dried by rotary evaporation for 2 h. Pellet was resuspended at 2 mg/ml in 25% 2-propanol, 25% acetonitrile, 50% dH_2O, 10% TFA to separate the glycan chains from the peptides by differential precipitation. The tube was vortexed thoroughly, sonicated, and placed on ice for 15 min. After centrifugation at 13,000 rpm for 15 min at 4 °C, the supernatant containing the stem-peptides and peptide bridges was transferred into a new tube and stored at −80 °C until further analysis. Before analysis, the frozen peptides were dried by overnight rotary evaporation and resuspended in 500 μl dH_2O. To separate the peptides, an HPLC system (Hitachi Instruments) consisting of an L-7200 autosampler, an L-7100 gradient pump, and an L-7400 UV detector was used as described previously (36). Aliquots of 100 μl were injected into a C18 reverse phase column (SuperPac Sephasil C18, 5 μm, 4 × 250-mm column, Amersham Pharmacia Biotech) maintained at 25 °C using a pelcooler (Lab-Source). A linear gradient of 0 to 15% acetonitrile in 0.1% trifluoroacetic acid at a flow rate of 0.5 ml/min over 100 min allowed separation of the peptides, which were detected at 210 nm. Collected data were analyzed with the D-7000 HPLC System Manager program (Hitachi).

Liquid chromatography coupled with mass spectrometry (LC-MS) analyses of the digested peptidoglycan

Peptidoglycan extraction was performed as described above. At the end of the digestion, samples were boiled at 100 °C to stop the enzymatic reaction. They were filtered through a 5000 MWCO cutoff column (Vivaspin 500, Sigma) and desalted using a C18 cartridge (Thermo Fisher). Peptidoglycan fragments were eluted with an 80% MeCN, 0.1% TFA solution and dried by rotary evaporation, before being dissolved in loading buffer (2% MeCN, 0.1% TFA). Samples were injected on a Dionex RSLC 3000 nanoHPLC system (Dionex) interfaced *via* a nanospray source with a high-resolution mass spectrometer QExactive Plus (Thermo Fisher). Peptidoglycan fragments were loaded onto a trapping microcolumn Acclaim PepMap100 C18 (20 mm × 100 μm ID, 5 μm, Dionex) before being separated on a C18 reversed-phase analytical nanocolumn at a flow rate of 0.25 μl/min. A Q-Exactive Plus instrument was interfaced with an Easy Spray C18 PepMap nanocolumn (50 cm × 75 μm ID, 2 μm, 100 Å, Dionex) using a gradient programmed to run over 37 min from 4 to 76% acetonitrile in 0.1% formic acid. Full mass spectrometry survey scans were performed at 70,000 resolution. In data-dependent acquisition controlled by Xcalibur software 3.1 (Thermo Fisher), the ten most intense multiply charged precursor ions detected in the full MS survey scan (250–2000 m/z window) were selected for higher energy collision-induced dissociation (HCD, normalized collision energy = 27%) and for analysis in the Orbitrap at 35,000 resolution. The window for precursor isolation was of 1.5 m/z units around the precursor and selected fragments were excluded from further analysis for 10 s. MS raw files were processed with PEAKS software (version 8.0, Bioinformatics Solutions Inc) and used for peptide identification by *de novo* sequencing and a database search. For the database search, a set of *S. dysgalactiae* (subspecies *equisimilis*) SK1249 proteome sequences was downloaded from the UniProt database (February 2016 version, 2309 sequences) and used to identify sample contamination by proteins from *S. dysgalactiae*. At the same time, *de novo* sequencing was used to identify peptidoglycan peptides. The database search and *de novo* sequencing parameters were as follows. No enzyme was used as the enzyme definition, N-terminal acetylation of protein and oxidation of methionine were used as variable modifications, and a parent ion tolerance of 10 ppm and a fragment ion mass tolerance of 0.02 Da were used.

ASBMB

Proteolytic degradation of the PlySK1249 endolysin in the presence of cell wall protein extracts and trypsin

Cell wall protein extracts from the strain *S. dysgalactiae* SK1249 were prepared, as described elsewhere (38). PlySK1249 and its truncated versions (40 μM) were digested overnight at 37 °C by mixing them with half volume of the extract. Additional endolysin samples were also digested by adding trypsin at 1 μg/ml for different incubation times. Digestions were conducted at 37 °C, 200 rpm agitation. When necessary, purified peptidoglycan was added to the reaction at a final concentration of 100 μg/ml. The reaction was stopped by incubating the mix with loading buffer and beta-mercaptoethanol for 15 min at 80 °C. The reaction products were loaded on a NuPAGE 4 to 12% BisTris gel. Bands of interest were cut from the gel and the amino acid sequences were determined by nanoLC-MS/MS. Briefly, bands were digested by trypsin, as described (39) and peptide analyzed as above on a Q-Exactive Plus instrument. MS/MS data were processed with Mascot 2.6 (Matrix Science) set up to search the *S. dysgalactiae* proteome in the UniProt database (reference proteome of *S. dysgalactiae* subsp. *equisimilis* (strain SK1249), August 2016 version: 2309 sequences). Trypsin (cleavage at K,R, excepted before P) was used as the enzyme definition with semi-specific cleavage, allowing two missed cleavages. Mascot was searched with a parent ion tolerance of 10 ppm and a fragment ion mass tolerance of 0.02 Da. Iodoacetamide derivative of cysteine was specified in Mascot as a fixed modification. N-terminal acetylation of protein and oxidation of methionine were specified as variable modifications.

Western blotting was performed as described previously (40) and blots were incubated for 1 h with a 1:1000 dilution of Anti-6xHis tag rabbit antibodies (Thermo Fisher Scientific) followed by a 1 h incubation with a 1:3000 dilution of goat anti-rabbit IgG coupled to HRP secondary antibodies (Thermo Fisher Scientific). Bands were detected by chemiluminescence using ECL Western blotting detection reagent (Amersham Bioscience). For fractionation of the cell wall protein extract, ammonium sulfate was used at multiple concentrations ranging from 15% to 100%. For each fractionation step, finely ground ammonium sulfate was added directly to 10 ml of cell wall extract and agitated for 15 min at 4 °C. The protein fractions were collected by centrifugation at 4000 rpm for 30 min. Pellets were resuspended in 100 μl PBS and mixed with 100 μl of the LysM_CHAP construct for overnight incubation. Western blotting was used to assess proteolyzed fragments in the different fractions, as described above. A second fractionation step was performed with 55% to 80% ammonium sulfate fractions loaded on a PBS-equilibrated size exclusion column (Superdex 200 Increase 10/300 GL, GE Healthcare). The protein content was eluted in 0.5 ml fractions with one column volume of PBS. Eluted fractions were tested for proteolytic activity using the LysM_CHAP construct, as described above. Four fractions were further analyzed by nanoLC-MS/MS. Briefly, fractions were digested by trypsin with a FASP (Filter-Aided Sample Preparation) protocol (41). Peptide were then analyzed by an Orbitrap Fusion Tribrid mass spectrometer (Thermo Scientific) and MS/MS data processed with Mascot 2.6, as described above. Scaffold software (version 4.8, Proteome Software Inc) was used to validate MS/MS-based protein and peptide identifications from Mascot searches and to perform data set alignment.

Endolysin proteolysis during in vivo prophage induction

For prophage induction, *S. dysgalactiae* strain FSL-S3-026 was grown at 37° in a synthetic CDEN medium (Amimed) to an OD_{600nm} of 0.2. Mitomycin was added at a final concentration of 1 μg/ml to induce prophage excision. After a 6 h induction, the culture was centrifuged, filtered at 0.22 μm, and concentrated to 1 ml using a Vivaspin turbo ultrafiltration unit (10 kDa MWCO, Sartorius AG). Samples were further concentrated to 50 μl after five successive washes using Tris 50 mM, pH 7.5 before being run on a 15% polyacrylamide SDS-PAGE gel. A total of five bands covering molecular weights ranging from 10 to 75 kDa were finally cut from the gel and peptides contained in each band were analyzed by nanoLC-MS/MS. Bands were digested by trypsin and peptide analyzed on a LTQ-Orbitrap Velos Pro instrument (Thermo Scientific). MS/MS data were processed with Mascot 2.6 set up to search the *Streptococcus agalactia* proteome in the UniProt database (reference proteome of *S. agalactia* (FSL S3-026 strain), June 2018 version: 2218 sequences). Trypsin (cleavage at K,R, excepted before P) was used as the enzyme definition with semi-specific cleavage, allowing two missed cleavages. Mascot was searched with a parent ion tolerance of 15 ppm and a fragment ion mass tolerance of 0.5 Da. Iodoacetamide derivative of cysteine was specified in Mascot as a fixed modification. N-terminal acetylation of protein and oxidation of methionine were specified as variable modifications. Scaffold software was used to validate MS/MS-based protein and peptide identifications from Mascot searches.

Endolysin diffusion assay

This assay was designed to assess the implication of the CBD in the diffusion of the endolysins through a layer of PBS soft-agar inoculated with bacteria. An overnight culture of *S. dysgalactiae* SK1249 was washed in PBS and resuspended in 0.25 vol of PBS. Granulated agar (7.5 g/l) was added to the cell suspension and autoclaved for 15 min at 120 °C. One ml/well of solution was poured into 6-well plates and stored at 4 °C until further use. 4 mm diameter wells were punched in the center of the agar surfaces and 10 μl aliquots of the enzyme at different concentrations were added into the pits. Diffusion was assessed by measuring the diameter of the lysis halo that formed after overnight incubation at 37 °C.

Data availability

The mass spectrometry proteomics data have been deposited to the ProteomeXchange Consortium *via* the PRIDE

(http://www.ebi.ac.uk/pride) partner repository with the data set identifier PXD024020.

Supporting information—This article contains supporting information.

Acknowledgments—The authors would like to thank Paul Majcherczyk for his outstanding technical help with the HPLC analysis, Patrice Waridel (Protein Analysis Facility, University of Lausanne, Switzerland) for performing all the LC-MS analyses, and Michael Taschner for helping with the size-exclusion chromatography experiments. We are grateful to Sara Mitri and Harald Brüssow for fruitful discussions, comments, and for reviewing the article.

Author contributions—F. O. conceived and supervised all the experiments, F. O. and C. M. performed the experiments, F. O. and P. M. wrote the article, G. R. corrected the article. All the authors provided critical feedback and helped shape the research, analysis, and article.

Funding and additional information—This work was supported by a nonrestricted grant from the Foundation for Advancement in Medical Microbiology and Infectious Diseases (FAMMID) (P. M.). This work was also supported by the Swiss National Science Foundation (SNSF) under grant P400PB_191059 (F.O).

Conflict of interest—The authors declare that they have no conflicts of interest with the contents of this article.

Abbreviations—The abbreviations used are: BHI, brain heart infusion; CBD, cell-wall-binding domain; CD, catalytic domain; IPTG, isopropyl β-D-1-thiogalactopyranoside; LB, lysogeny broth; PBS, phosphate-buffered saline; TEM, transmission electron microscopy.

References

1. Young, R. (2014) Phage lysis: Three steps, three choices, one outcome. *J. Microbiol.* **52**, 243–258
2. Nelson, D. C., Schmelcher, M., Rodriguez-Rubio, L., Klumpp, J., Pritchard, D. G., Dong, S., and Donovan, D. M. (2012) Endolysins as antimicrobials. *Adv. Virus Res.* **83**, 299–365
3. Fischetti, V. A. (2008) Bacteriophage lysins as effective antibacterials. *Curr. Opin. Microbiol.* **11**, 393–400
4. Fischetti, V. A. (2010) Bacteriophage endolysins: A novel anti-infective to control gram-positive pathogens. *Int. J. Med. Microbiol.* **300**, 357–362
5. Schleifer, K. H., and Kandler, O. (1972) Peptidoglycan types of bacterial cell walls and their taxonomic implications. *Bacteriol. Rev.* **36**, 407–477
6. Vollmer, W., Blanot, D., and de Pedro, M. A. (2008) Peptidoglycan structure and architecture. *FEMS Microbiol. Rev.* **32**, 149–167
7. Horgan, M., O'Flynn, G., Garry, J., Cooney, J., Coffey, A., Fitzgerald, G. F., Ross, R. P., and McAuliffe, O. (2009) Phage lysin LysK can be truncated to its CHAP domain and retain lytic activity against live antibiotic-resistant staphylococci. *Appl. Environ. Microbiol.* **75**, 872–874
8. Wang, X., Wilkinson, B. J., and Jayaswal, R. K. (1991) Sequence analysis of a Staphylococcus aureus gene encoding a peptidoglycan hydrolase activity. *Gene* **102**, 105–109
9. Gu, J., Xu, W., Lei, L., Huang, J., Feng, X., Sun, C., Du, C., Zuo, J., Li, Y., Du, T., Li, L., and Han, W. (2011) LysGH15, a novel bacteriophage lysin, protects a murine bacteremia model efficiently against lethal methicillin-resistant Staphylococcus aureus infection. *J. Clin. Microbiol.* **49**, 111–117
10. O'Flaherty, S., Coffey, A., Meaney, W., Fitzgerald, G. F., and Ross, R. P. (2005) The recombinant phage lysin LysK has a broad spectrum of lytic activity against clinically relevant staphylococci, including methicillin-resistant Staphylococcus aureus. *J. Bacteriol.* **187**, 7161–7164
11. Navarre, W. W., Ton-That, H., Faull, K. F., and Schneewind, O. (1999) Multiple enzymatic activities of the murein hydrolase from staphylococcal phage phi11. Identification of a D-alanyl-glycine endopeptidase activity. *J. Biol. Chem.* **274**, 15847–15856
12. Rashel, M., Uchiyama, J., Ujihara, T., Uehara, Y., Kuramoto, S., Sugihara, S., Yagyu, K., Muraoka, A., Sugai, M., Hiramatsu, K., Honke, K., and Matsuzaki, S. (2007) Efficient elimination of multidrug-resistant Staphylococcus aureus by cloned lysin derived from bacteriophage phi MR11. *J. Infect. Dis.* **196**, 1237–1247
13. Pritchard, D. G., Dong, S., Baker, J. R., and Engler, J. A. (2004) The bifunctional peptidoglycan lysin of Streptococcus agalactiae bacteriophage B30. *Microbiology (Reading)* **150**, 2079–2087
14. Pritchard, D. G., Dong, S., Kirk, M. C., Cartee, R. T., and Baker, J. R. (2007) LambdaSa1 and LambdaSa2 prophage lysins of Streptococcus agalactiae. *Appl. Environ. Microbiol.* **73**, 7150–7154
15. Donovan, D. M., and Foster-Frey, J. (2008) LambdaSa2 prophage endolysin requires Cpl-7-binding domains and amidase-5 domain for antimicrobial lysis of streptococci. *FEMS Microbiol. Lett.* **287**, 22–33
16. Hyman, P., and Abedon, S. (2012) *Bacteriophages in Health and Disease*, CABI Press, Wallingford, UK
17. Low, L. Y., Yang, C., Perego, M., Osterman, A., and Liddington, R. (2011) Role of net charge on catalytic domain and influence of cell wall binding domain on bactericidal activity, specificity, and host range of phage lysins. *J. Biol. Chem.* **286**, 34391–34403
18. Wong, J. E., Midtgaard, S. R., Gysel, K., Thygesen, M. B., Sorensen, K. K., Jensen, K. J., Stougaard, J., Thirup, S., and Blaise, M. (2015) An intermolecular binding mechanism involving multiple LysM domains mediates carbohydrate recognition by an endopeptidase. *Acta Crystallogr. D Biol. Crystallogr.* **71**, 592–605
19. Visweswaran, G. R., Leenhouts, K., van Roosmalen, M., Kok, J., and Buist, G. (2014) Exploiting the peptidoglycan-binding motif, LysM, for medical and industrial applications. *Appl. Microbiol. Biotechnol.* **98**, 4331–4345
20. Loessner, M. J. (2005) Bacteriophage endolysins–current state of research and applications. *Curr. Opin. Microbiol.* **8**, 480–487
21. Buist, G., Steen, A., Kok, J., and Kuipers, O. P. (2008) LysM, a widely distributed protein motif for binding to (peptido)glycans. *Mol. Microbiol.* **68**, 838–847
22. Loessner, M. J., Kramer, K., Ebel, F., and Scherer, S. (2002) C-terminal domains of Listeria monocytogenes bacteriophage murein hydrolases determine specific recognition and high-affinity binding to bacterial cell wall carbohydrates. *Mol. Microbiol.* **44**, 335–349
23. Donovan, D. M., Foster-Frey, J., Dong, S., Rousseau, G. M., Moineau, S., and Pritchard, D. G. (2006) The cell lysis activity of the Streptococcus agalactiae bacteriophage B30 endolysin relies on the cysteine, histidine-dependent amidohydrolase/peptidase domain. *Appl. Environ. Microbiol.* **72**, 5108–5112
24. Becker, S. C., Dong, S., Baker, J. R., Foster-Frey, J., Pritchard, D. G., and Donovan, D. M. (2009) LysK CHAP endopeptidase domain is required for lysis of live staphylococcal cells. *FEMS Microbiol. Lett.* **294**, 52–60
25. Oechslin, F., Daraspe, J., Giddey, M., Moreillon, P., and Resch, G. (2013) *In vitro* characterization of PlySK1249, a novel phage lysin, and assessment of its antibacterial activity in a mouse model of Streptococcus agalactiae bacteremia. *Antimicrob. Agents Chemother.* **57**, 6276–6283
26. Herbold, D. R., and Glaser, L. (1975) Interaction of N-acetylmuramic acid L-alanine amidase with cell wall polymers. *J. Biol. Chem.* **250**, 7231–7238
27. Rigden, D. J., Jedrzejas, M. J., and Galperin, M. Y. (2003) Amidase domains from bacterial and phage autolysins define a family of gamma-D,L-glutamate-specific amidohydrolases. *Trends Biochem. Sci.* **28**, 230–234
28. Fan, D. P. (1970) Autolysin(s) of Bacillus subtilis as dechaining enzyme. *J. Bacteriol.* **103**, 494–499
29. Layec, S., Gerard, J., Legue, V., Chapot-Chartier, M. P., Courtin, P., Borges, F., Decaris, B., and Leblond-Bourget, N. (2009) The CHAP domain of Cse functions as an endopeptidase that acts at mature septa to promote Streptococcus thermophilus cell separation. *Mol. Microbiol.* **71**, 1205–1217
30. Steen, A., Palumbo, E., Deghorain, M., Cocconcelli, P. S., Delcour, J., Kuipers, O. P., Kok, J., Buist, G., and Hols, P. (2005) Autolysis of Lactococcus

lactis is increased upon d-alanine depletion of peptidoglycan and lipoteichoic acids. *J. Bacteriol.* **187**, 114–124
31. Buist, G., Venema, G., and Kok, J. (1998) Autolysis of Lactococcus lactis is influenced by proteolysis. *J. Bacteriol.* **180**, 5947–5953
32. Eckert, C., Lecerf, M., Dubost, L., Arthur, M., and Mesnage, S. (2006) Functional analysis of AtlA, the major N-acetylglucosaminidase of Enterococcus faecalis. *J. Bacteriol.* **188**, 8513–8519
33. Christensen, J. E., Dudley, E. G., Pederson, J. A., and Steele, J. L. (1999) Peptidases and amino acid catabolism in lactic acid bacteria. *Antonie Van Leeuwenhoek* **76**, 217–246
34. Steen, A., Buist, G., Horsburgh, G. J., Venema, G., Kuipers, O. P., Foster, S. J., and Kok, J. (2005) AcmA of Lactococcus lactis is an N-acetylglucosaminidase with an optimal number of LysM domains for proper functioning. *FEBS J.* **272**, 2854–2868
35. Broskey, N. T., Daraspe, J., Humbel, B. M., and Amati, F. (2013) Skeletal muscle mitochondrial and lipid droplet content assessed with standardized grid sizes for stereology. *J. Appl. Physiol.* **115**, 765–770
36. Majcherczyk, P. A., Langen, H., Heumann, D., Fountoulakis, M., Glauser, M. P., and Moreillon, P. (1999) Digestion of Streptococcus pneumoniae cell walls with its major peptidoglycan hydrolase releases branched stem peptides carrying proinflammatory activity. *J. Biol. Chem.* **274**, 12537–12543
37. Schmelcher, M., Shen, Y., Nelson, D. C., Eugster, M. R., Eichenseher, F., Hanke, D. C., Loessner, M. J., Dong, S., Pritchard, D. G., Lee, J. C., Becker, S. C., Foster-Frey, J., and Donovan, D. M. (2015) Evolutionarily distinct bacteriophage endolysins featuring conserved peptidoglycan cleavage sites protect mice from MRSA infection. *J. Antimicrob. Chemother.* **70**, 1453–1465
38. Que, Y. A., Haefliger, J. A., Francioli, P., and Moreillon, P. (2000) Expression of Staphylococcus aureus clumping factor A in Lactococcus lactis subsp. cremoris using a new shuttle vector. *Infect. Immun.* **68**, 3516–3522
39. Shevchenko, A., Tomas, H., Havlis, J., Olsen, J. V., and Mann, M. (2006) In-gel digestion for mass spectrometric characterization of proteins and proteomes. *Nat. Protoc.* **1**, 2856–2860
40. Towbin, H., Staehelin, T., and Gordon, J. (1979) Electrophoretic transfer of proteins from polyacrylamide gels to nitrocellulose sheets: Procedure and some applications. *Proc. Natl. Acad. Sci. U. S. A.* **76**, 4350–4354
41. Wisniewski, J. R., Zougman, A., Nagaraj, N., and Mann, M. (2009) Universal sample preparation method for proteome analysis. *Nat. Methods* **6**, 359–362